JOURNAL OF AGRICULTURAL AND FOOD CHEMISTRY

Deposition of Cell Wall Polysaccharides in Wheat Endosperm during Grain Development: Fourier Transform-Infrared Microspectroscopy Study

SULLY PHILIPPE,† PAUL ROBERT,† CÉCILE BARRON,‡ LUC SAULNIER,† AND FABIENNE GUILLON*,†

Unité de Recherches Biopolymères, Interactions et Assemblages, INRA, BP 71627, 44316 Nantes, and Unité Mixte de Recherches Ingénierie des Agropolymères et Technologies Emergentes, INRA-ENSAM-UMII-CIRAD, 2 place Viala, 34060 Montpellier, France

The time course and pattern deposition of the cell wall polysaccharides in the starchy endosperm of wheat (*Triticum aestivum* cv. Recital) during grain development was studied using Fourier transform infrared microspectroscopy (micro-FTIR). Three stages of grain development identified as key stages for cell wall construction were retained as follows: the end cellularization, the beginning of cell differentiation, and the beginning of maturation. Micro-FTIR revealed that β-(1→3),(1→4) glucans and arabinoglactan proteins are the main cell wall components of endosperm at the end of the cellularization stage, whereas arabinoxylans (AX) appeared only at the cell differentiation stage. Past the differentiation stage, FTIR spectra were dominated by AX features. Cell walls at the beginning of cell differentiation and at endosperm maturation could be distinguished by spectral features that were ascribed to AX substitution. AX appeared more substituted at the beginning of cell differentiation. Moreover, a difference in the degree of AX substitution was found between peripheral and central parts of the grain at the cell differentiation stage; AX in central cells was less substituted. Thus, dramatic changes in endosperm cell wall composition were detected during wheat grain development with respect to both the relative occurrence of individual constituents and the fine structure of the AX.

KEYWORDS: Arabinoxylans; endosperm; FTIR; β-(1→3),(1→4) glucans; immunolabeling; principal component analysis; *Triticum aestivum*

INTRODUCTION

Cell walls in wheat grain endosperm account for 2−4% of dry weight and have a significant effect on wheat grain uses such as milling, baking, and brewing and in animal feeding or human nutrition (*1*). Arabinoxylans (AXs) are the main non-starch polysaccharides of cell walls of mature wheat grain endosperm (70% w/w) (*1*). AXs comprise chains of (1→4)-linked β-D-xylopyranose residues in which a proportion of the individual xylopyranose residues are substituted at either the O-3 or both the O-2 and the O-3 positions with terminal α-L-arabinofuranose. Few arabinose residues are esterified with ferulic acid, and some AX molecules can be cross-linked through dehydroferulate bridges in walls (*2*, *3*). Differences in the chain length of the xylan backbone and in the proportion of xylose residues substituted with arabinose were observed between AX issued from different cultivars (*4*, *5*) of wheat and from different parts of the grain (*4*−*7*). As a matter of fact, structural changes are often characterized by the arabinose-to-xylose ratio (A/X). This ratio ranges from 0.3 to 0.4 in aleurone walls (*8*−*10*) and from 0.5 to 0.6 in starchy endosperm walls (*4*). Other components involved in endosperm cell walls are β-(1→3),(1→4) glucans (20−29% w/w) with minor amounts of glucomannans (2−7% w/w) and cellulose (2−4% w/w) (*8*, *11*). β-(1→3),(1→4) glucans are found in higher proportion in cell walls of the aleurone and subaleurone layer than in the starchy endosperm (*12*, *13*). Arabinogalactan proteins (AGPs) often assimilated as wall components (*14*) accounted for 0.3% w/w of flour (*15*).

The impact of cell wall composition and AX structural changes on cell wall properties and therefore on wheat grain uses is not fully understood. Although cell wall components of mature grains have been largely characterized, the basic understanding of their occurrence and distribution across the endosperm is still lacking. The ability to improve wheat grain uses through supervising cell wall properties is consequently limited.

* To whom correspondence should be addressed. Tel: +33-2-40675016. Fax: +33-2-40675229. E-mail: guillon@nantes.inra.fr.
† Unité de Recherches Biopolymères, Interactions et Assemblages.
‡ Unité Mixte de Recherches Ingénierie des Agropolymères et Technologies Emergentes.

10.1021/jf052922x CCC: $33.50
Published on Web 02/24/2006

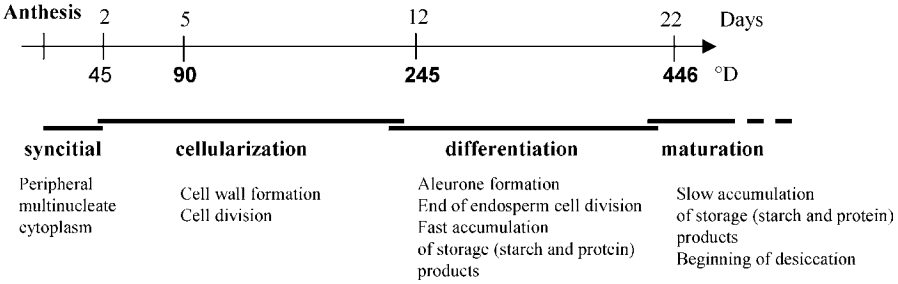

Figure 1. Time course of wheat grain development. Four stages of wheat grain development are distinguished according to the events that affect the endosperm since anthesis (*26*–*29*). °D, temperature/energy cumulated daily by the grain after anthesis.

The endosperm develops in four stages (**Figure 1**) (*16*−*19*). The first stage corresponds to the syncitial period (0−2/3 days after anthesis, DAA) and is characterized by nuclei division inside the embryo sac. At this stage, no cell walls are formed. During the cellularization period (stage 2, 2/3 DAA to 12/14 DAA), the nuclei of endosperm continue to quickly divide and cell walls start to grow near the inner nucellar epidermis. By about 8 days, cellularization is completed. The proliferation of cells by division goes on for several days (until 16 DAA). The next stage (stage 3, 12/14 to 21/23 DAA) corresponds to cell differentiation, a period for cell expansion in which the water content increases and starch and protein reserves accumulate. At this stage, the aleurone layer appears. At the maturation stage (stage 4, 21/23 to 31 DAA), storage protein and starch have been accumulated in the endosperm. The fresh weight of kernels declines as water is lost and the starchy endosperm cells die.

Immunochemical approaches have been used to investigate AX distribution in mature and developing wheat grain endosperm (*20*, *21*). Antibodies against unsubstituted and low substituted regions of AX have been produced and used. In mature grain, AXs were detected in all cell walls of the endosperm, with some differences in the labeling pattern according to endosperm cell type. The antibodies against unsubstituted regions of AX reacted less with the subaleurone cell walls than with the starchy endosperm cells. During grain development, poor substituted AXs were detected at the beginning of cell differentiation (*21*). While cell walls mainly contained β-(1→3) glucans at the cellularization stage, no β-(1→3) glucans were observed past cellularization. Instead, β-(1→3),(1→4) glucans were found equally distributed in all thin walls of the endosperm. At the end of grain filling, cell walls looked similar to those of mature endosperm. Philippe et al. (*21*) reported distinct patterns in the peripheral and central starchy endosperm but could not conclude on the degree of substitution of AX. Vibrational microspectroscopy methods are complementary to immunochemical approaches and have been used to study changes of endosperm cell wall composition in mature and developing wheat grains in relation with grain cohesion and hardness (*22*−*24*). Piot et al. (*23*) using Raman microspectroscopy reported that endosperm walls consisted of not only AX esterified with ferulic acid but also small amounts of proteins and lipids. They found that during wheat grain maturation, the ferulic acid content evolved in starchy endosperm cell walls. Unfortunately, the authors did not pay attention to the heterogeneity of cell wall composition across the endosperm at a given stage of development. Barron et al. (*24*) using Fourier transform infrared microspectroscopy (micro-FTIR) reported compositional differences between peripheral and central starchy endosperm cell walls regardless of the cultivars studied. They ascribed the differences to AX.

The purpose of the present work was to precisely confirm the information obtained on the time course and pattern of polysaccharides deposition in cell walls during wheat grain development. Three stages of grain development identified as key stages for cell wall construction (*21*) were retained as follows: the end cellularization, the beginning of cell differentiation, and the beginning of endosperm maturation. Micro-FTIR has been shown to be powerful for investigating the composition of cell walls in their native form (*25*−*29*), and recently, the assignment of AX infrared spectrum was made clearer (*26*). In particular, the absorption bands at 984 and 958 cm^{-1} were found to be indicative of the degree of substitution of AX. It was also shown using model mixtures that AX, β-(1→3)(1→4) glucans and AGPs could be distinguished on the basis of their spectral signature. In the present study, micro-FTIR has been used coupled with a multivariate statistical method. Particular emphasis was put on AXs and their degrees of substitution.

MATERIALS AND METHODS

Biological Materials. *Triticum aestivum* cv. Recital, a winter common wheat, was grown in a glasshouse under conditions of natural day length (UMR Amélioration des Plantes et Biotechnologies Végétales, INRA, Rennes, France). The wheat seedlings were vernalized for 2 months in a growth cabinet at 8 °C; light, 8 h, and dark, 16 h. Seedlings were then transplanted into individual pots using a standard potting mixture (peat RHP15 Klassman, K Klasmann France, Bourgoin Jaillieu, France). After planting, an Osmocote (R) Exact Tablet containing nitrogen (15%), phosphate (9%), potassium hydroxide (9%), and magnesium (3%) (Scotts International B. V., Waardenburg, The Netherland) was added. The plants were watered daily. Following anthesis, the mean daily temperatures were recorded and thermal times (degree days, °D) were calculated as the summation of the mean daily temperatures since anthesis minus the base temperature. The base temperature used was 0 °C (*31*). Grains were harvested at three different stages of development: 90 (end of endosperm cellularization), 245 (beginning of cell differentiation), and 446 °D (beginning of maturation) (**Figure 1**).

FTIR Microspectroscopy. *Samples Preparation.* Wheat grains were picked up from the middle third of ears and stored in 70% ethanol. Sectioning was carried out with a Vibratome (Microm Microtech, France) in 70% ethanol. Transverse sections, 50 μm thick, were sonicated in 70% ethanol for 2 min to remove cell contents. The sections were thereafter washed in 70% ethanol. The procedure developed by Barron et al. (*24*) produced transverse sections of the grain consisting of cell walls whose chemical composition was as close as possible to that in the original grain. No resin embedding or thermal or enzymatic treatments were used.

FTIR Analysis. Sections laid down onto barium fluoride disks were dried at room temperature. The starchy endosperm cell walls prepared in this way became flat, less than 10 μm thick, and therefore suitable for analysis by micro-FTIR. Unfortunately, the aleurone layer after drying remained too thick for micro-FTIR study.

Infrared spectra were collected in the transmission mode, between 750 and 4000 cm^{-1} at 4 cm^{-1} intervals, using a Magna-IR 550 spectrometer (Nicolet, Trappes, France) equipped with an IR-plan

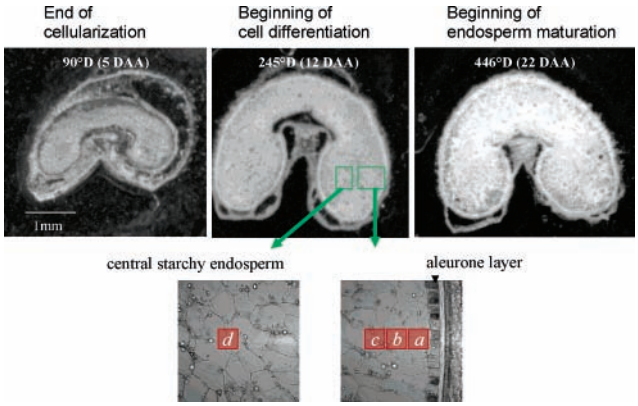

Figure 2. (**A**) Transverse sections of wheat grain endosperm (*Triticum aestivum*) at the three development stages considered for the present study. (**B**) Light microscope image of wheat grain section at 245 °D (beginning of cell differentiation) after sonication showing the network of endosperm cell walls. Zones were noted a–c for the starchy endosperm peripheral regions and d corresponding to the endosperm central region.

Advantage microscope (Spectra-Tech, Shelton,CT; ×15 Reflachromat lens). The spectrometer was fitted with a high-sensitivity MCT detector. Each spectrum resulted from the coaddition of 200 scans. The 935−1020 cm^{-1} spectral region was further smoothed, and baselines were corrected and normalized using the OPUS-NT softtware (Version 2.06, Bruker, France). Second derivative spectral data were assessed in order to enhance spectral differences in the 1020−935 cm^{-1} region. The second derivative data were obtained by using the Savitzky−Golay algorithm (*32*), developed on the OPUS-NT (Bruker) software.

In preliminary experiments, infrared spectra were recorded for the peripheral and central regions (80 × 80 μm^2) of 10 different grains at 245 °D. The spectral data revealed differences according to the regions but no grain effect. For each stage of development, three grains were therefore considered in the following studies. Four zones of 80 × 80 μm^2 were investigated for each section (**Figure 2**). Zones were noted a−c for the starchy endosperm peripheral region and d corresponding to the endosperm central region.

Data Treatment. Principal component analysis (PCA) was applied to the second derivative spectral data (*33*, *34*). This multivariate data treatment made it possible to handle large data tables without making any preliminary assumptions. The computation of principal components is based on the diagonalization of the variance−covariance matrix **V** assessed from the spectral data **X**. The diagonalization realizes a decomposition of **V** into eigenvectors **L** and eigenvalues **S**. The eigenvalues describe the amount of total variance taken into account by the principal components. The eigenvectors are used to assess the principal component scores **C**.

$$\mathbf{V} = \mathbf{X}'\mathbf{X}$$

$$\mathbf{C} = \mathbf{XL}$$

where **X** is the matrix of the spectral data (*n* samples × *m* wavenumbers) and **X′** is the transpose matrix of **X**.

The principal component scores were used to draw similarity maps that allowed a comparison of the spectra to each other. Characteristic absorption bands were depicted using the spectral patterns derived from the eigenvectors.

RESULTS AND DISCUSSION

Spectral Behavior of Wheat Endosperm. Figure 2 shows the transverse sections of wheat endosperm at the three developmental stages. Spectra of starchy endosperm at 90, 245, and 446 °D (**Figure 3**) showed broad absorption bands for polysaccharides between 1200 and 800 cm^{-1} (*35*−*37*). All spectra presented a maximum absorption band at about 1040 cm^{-1} that might be assigned to C−OH bending, with shoulders

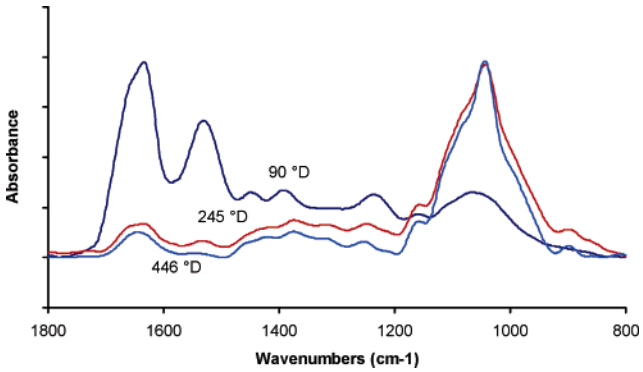

Figure 3. Micro-FTIR spectra of endosperm cell walls at 90 (end of cellularization), 245 (beginning of cell differentiation), and 446 °D (beginning of endosperm maturation). Spectra shown were recorded in the central region (zone d) of grain.

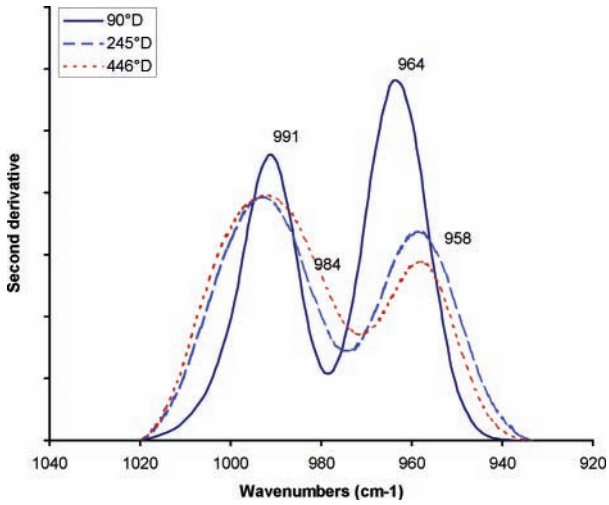

Figure 4. Micro-FTIR spectra of central starchy endosperm (zone d) at 90 (end of cellularization), 245 (beginning of cell differentiation), and 446 °D (beginning of endosperm maturation). Second derivative spectra of the 1020–935 cm^{-1} region for AX, β-(1→3),(1→4) glucans, and AGPs. Second derivative data calculated using the Savitzky–Golay algorithm (*31*) were multiplied by –1.

at 1070 and 985 cm^{-1}. The absorption band around 1150 cm^{-1} was assigned to glycosidic linkages while the band at 890 cm^{-1} was characteristic of β-(1→4) linkages. The absence of band at 1033 cm^{-1} indicated that cellulose was absent or at low concentrations. Some proteins remained as suggested by the presence of absorption bands at 1640 and 1550 cm^{-1}. In particular, protein absorption bands were remarkably intense at 90 °D.

Temporal Deposition of Wall Polymers. Spectra of the four starchy endosperm zones at 90, 245, and 446 °D were compared. The 1020−935 cm^{-1} region, specific of the main polysaccharides from wheat endosperm (*38*), was investigated. Spectra at 245 and 446 °D were almost superimposed and showed only tiny differences (data not shown). A careful examination of the spectra was therefore carried out by assessing second derivative spectral data. **Figure 4** shows the second derivative spectra for the central region (zone d) of wheat endosperm. Spectra recorded at 90 °D differed from those obtained at 245 and 446 °D. At 90 °D, strong absorption bands were observed at 991 and 964 cm^{-1} that might be assigned to β-(1→3)(1→4) glucans and AGPs, respectively (*30*). At 245 and 446 °D, two broad bands centered at 991 and 958 cm^{-1} were revealed. While the absorption band centered at 991 cm^{-1} characterized the presence

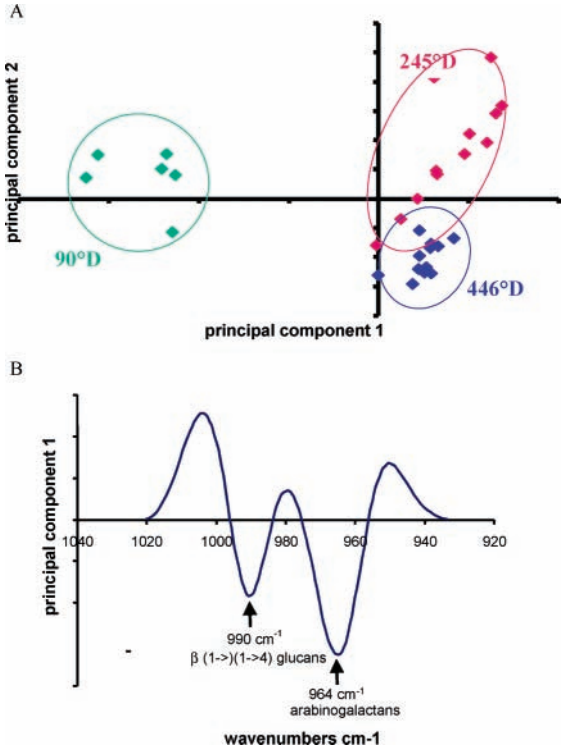

Figure 5. PCA applied to the whole data set. (**A**) Similarity map of micro-FTIR spectra (second derivative of the 1020–935 cm^{-1} region) at 90 (end of cellularization), 245 (beginning of cell differentiation), and 446 °D (beginning of endosperm maturation). The spectral features of starchy endosperm at 245 and 446 °D could be clearly distinguished from those of the endosperm at 90 °D along principal component one. (**B**) Spectral pattern obtained from the first PCA loading, showing influent wavenumbers for the discrimination of stages.

of β-(1→3)(1→4) glucans, the band at 958 cm^{-1} was assigned to AX (*30*). The comparison of the 245 and 446 °D infrared spectra showed that a decrease of the intensity at 958 cm^{-1} was accompanied by an increase of a shoulder at 984 cm^{-1}. Using purified AX and model xylo-oligosaccharides with varying degrees of substitution (*30*), it has been shown that these two bands are sensitive to arabinosyl substitution: Whereas the intensity of the band at 958 cm^{-1} increased with the degree of substitution, that at 984 cm^{-1} decreased.

PCA was applied to all second derivative spectra. The first two principal components took 58 and 36% of the total inertia into account (**Figure 5A**). Samples at the early stage of endosperm development (90 °D) were identified by negative scores along principal component 1, whatever the endosperm region. All spectra collected at 245 and 446 °D were characterized by positive scores for principal component 1. The loading plot associated with principal component 1 made it possible to explore the spectral features that discriminated the samples (**Figure 5B**). The spectral pattern or loading plot revealed negative peaks at 991 and 964 cm^{-1} that corresponded to β-(1→3),(1→4) glucans and AGPs, respectively. Positive peaks at about 1002, 984, and 956 cm^{-1} were assigned to AX. In other words, FTIR spectra revealed that β-(1→3),(1→4) glucans and AGPs are the main cell wall components of endosperm at the early stage of grain development, whereas AX appeared only at 245 °D (beginning of cell differentiation stage). Past the differentiation stage, FTIR spectra were dominated by AX features.

Specific antibodies have already shown the early deposit of β-(1→3),(1→4) glucans (*21*) in endosperm during grain development. In mature wheat, β-(1→3),(1→4) glucans are present in mature wheat grain but not as the major cell wall polymer (*11*−*13*, *20*). In barley endosperm, the first evidence of β-(1→3),(1→4) glucans is found at 17 DAA although the greatest accumulation occurs from 23 DAA onward (*39*). In vegetative organs, they have been described as polysaccharides specific of the developmental stage (*40*, *41*). In elongating maize coleoptiles, β-(1→3),(1→4) glucans are supposed to coat cellulose microfibrils and to participate in the control of cell wall extension during growth (*40*). Therefore, β-(1→3),(1→4) glucans may act as structural elements of the walls in growing cells at early stages of wheat development. In addition, β-(1→3),(1→4) glucans are thought to be an endosperm storage material hydrolyzed during germination of grain (*42*).

Using micro-FTIR, AGPs were detected in wheat grain only at the end of the cellularization stage. Biochemical analyses indicated that AGPs are also present in mature grain (*15*). The absence of AGPs past to 90 °D using micro-FTIR could be due to a high amount of AX overlapping absorption bands of AGPs. A number of roles have been suggested for AGPs, including involvement in morphogenesis, cell proliferation, programmed cell death, and germination as available storage material (*14*).

Accumulation of AX took place at the beginning of the differentiation stage (245 °D). Results obtained using micro-FTIR were in agreement with previous data obtained using immunocytochemistry (*21*). At this stage of development, the final length of the grain is almost reached, and starch and protein accumulation are initiated. The synthesis of AX could correspond to the fixation of the wall structure at this stage of development. AX might be specifically involved in the strengthening of walls through interactions with β-(1→3),(1→4) glucans (*43*). Alternatively, strengthening could be mediated by association of AX chains through the formation of dehydroferulate bridges (*2*, *3*).

Structural Heterogeneity of AX during Grain Development. A second PCA was applied to the second derivative spectra recorded at 245 and 446 °D to study changes in the degree of substitution of AX (A/X). The two stages of development are clearly identified along principal component 1 (**Figure 6A**). In addition, the outer zones a and b could be distinguished from the central zone d at 245 °D. Principal component 1 (83% of the total inertia) resulted from an opposition between peaks at 984 and 958 cm^{-1} (**Figure 6B**). Robert et al. (*30*) have shown that the increase of the intensity peak at 958 cm^{-1}, accompanied by a decrease at 984 cm^{-1}, characterized the presence of highly substituted AX. Consequently, AX seemed to be more substituted at 245 than at 446 °D. At 245 °D, AX in peripheral cells (zones a and b) appeared more substituted than AX in central cells (zone d).

The decrease in AX substitution during grain development may result from an alteration of highly substituted AX after deposition in wall due to the action of AX arabinofuranohydrolases. Such an enzyme has been purified from barley developing seedlings (*44*). AX remodeling has been previously reported during barley coleoptile growth and development (*45*). It has been suggested that the high degree of arabinosyl substitution of newly synthesized AX promotes their solubility and transport through the endomembrane system (*46*). As cell walls mature, removing arabinose residues could lead to a decrease of solubility. The newly unsubstituted regions generated in AX could stiffen cell walls through hydrogen-bonding interactions with other cell wall polysaccharides (*43*). Intermediate stages of development between 245 and 446 °D must be investigated to allow more confident conclusions to be drawn,

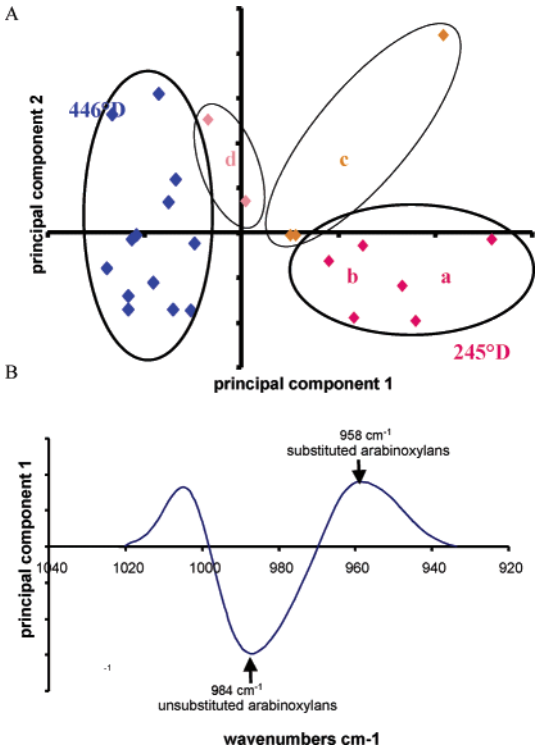

Figure 6. PCA applied to spectra from starchy endosperm at 245 (beginning cell differentiation) and 446 °D (beginning of endosperm maturation), taking into account location within the starchy endosperm. (**A**) Similarity map of micro-FTIR spectra (second derivative of the 1020–935 cm^{-1} region). a–c are adjacent areas in the peripheral region of the starchy endosperm, and d is the endosperm central region. Clustering according to the stage of development was obtained along the principal component one. The most external areas (a, b) and central region (zone d) of the starchy endosperm at 245 °D were also contrasted. (**B**) Spectral pattern obtained from the first PCA loading, showing influent wavenumbers for the discrimination of stages and endosperm zones.

regarding AX remodeling. Complementary experiments using antibodies specific of highly substituted regions of AX and enzymatic fingerprinting could clarify changes in AX substitution.

Using specific antibodies against unsubstituted and low substituted AX, different labeling was observed between peripheral and central cells at 245 and 446 °D (*21*). However, it was not possible to conclude whether the epitope accessibility, the AX content, or its structure was responsible for labeling differences. Spatial heterogeneity in the composition of cell walls between peripheral and central starchy endosperm regions has been observed using micro-FTIR without relating the differences to AX substitution (*24*). The outer region in mature grain starchy endosperm mainly consists of cells containing low starch and high storage protein contents. The present paper indicated that outer cell walls were characterized by highly substituted AX. This supports the hypothesis that gene expression profiles could differ according to cell position (*47*), resulting in compositional differences across the endosperm.

In the present study, a conventional thermal infrared source and an aperture size of 80 × 80 μm^2 were used. As a consequence, spectral data were from large areas and could not reveal chemical features within cellular dimensions. However, application of PCA to spectral data made it possible to confirm immunochemical results on time course and pattern deposition of the β-(1→3)(1→4) glucans and AX. The use of a synchrotron source, thanks to its brightness, will permit us to get more precise information on cell wall composition at the cellular scale (*48*, *49*).

ABBREVIATIONS USED

AX arabinoxylans, A/X molar ratio of arabinose to xylose; AGPs, arabinogalactan proteins; DAA, days after anthesis; mAb, monoclonal antibody; pAb, polyclonal serum; PCA, principal component analysis; micro-FTIR, Fourier transform microspectroscopy; WE, water extractable.

LITERATURE CITED

(1) Fincher, G. B.; Stone, B. A. Cell walls and their components in cereal grain technology. In *Advances in Cereal Science and Technology*; Pomeranz, Y., Ed.; American Association of Cereal Chemists: St. Paul, MN, 1986; pp 207−295.
(2) Ralph, J.; Quideau, S.; Grabbern, J. H.; Hatfield, R. D. Identification and synthesis of new ferulic dehydromers present in grass cell walls. *J. Chem. Soc.* **1994**, *1*, 3485−3498.
(3) Ishii, T. Structure and function of feruloylated polysaccharides. *Plant Sci.* **1997**, *127*, 111−127.
(4) Ordaz-Ortiz, J. J.; Saulnier, L. Structural variability of arabinoxylans from wheat flours. Comparison of water-extractable and xylanase-extractable arabinoxylans. *J. Cereal Sci.* **2005**, *42*, 119−125.
(5) Ordaz-Ortiz, J. J.; Devaux, M. F.; Saulnier, L. Classification of wheat varieties based on structural features as arabinoxylans as revealed by endoxylanase treatment of flour and grain. *J. Agric. Food Chem.* **2005**, *53*, 8349−8356.
(6) Andersson, R.; Westerlund, E.; Aman, P. Natural variations in the contents of structural elements of water-extractable nonstarch polysaccharides in white flour. *J. Cereal Sci.* **1994**, *19*, 77−82.
(7) Delcour, J. A.; Van Win, H.; Grobet, P. J. Distribution and structural variation of arabinoxylans in common wheat mill streams. *J. Agric. Food Chem.* **1999**, *47*, 271−275.
(8) Bacic, A.; Stone, B. A. Isolation and ultrastructure of cell walls from wheat and barley. *Aust. J. Plant Physiol.* **1981**, *8*, 453−474.
(9) Rhodes, D. I.; Sadek, M.; Stone, B. A. Hydroxycinnamic acids in walls of wheat aleurone cells. *J. Cereal Sci.* **2002**, *36*, 67−81.
(10) Antoine, C.; Peyron, S.; Mabille, S.; Lapierre, C.; Bouchet, C.; Abecassis, J.; Rouau, X. Individual contribution of grain outer layers and their cell wall structure to the mechanical properties of wheat bran. *J. Agric. Food Chem.* **2003**, *51*, 2026−2033.
(11) Mares, D. J.; Stone, B. A. Studies on wheat endosperm. I. Chemical composition and ultrastructure of the cell walls. *Aust. J. Plant Physiol.* **1973**, *26*, 793−812.
(12) Beresford, G.; Stone, B. A. (1-3,1-4)-β-D-glucan content of *Triticum* grains. *J. Cereal Sci.* **1983**, *1*, 111−114.
(13) Fulcher, R. G.; Miller, S. S.; Ruan, R. Quantitative microscopic approaches to carbohydrate characterization and distribution in cereal grains. In *Functionality of Food Phytochemicals*; Johns, R., Ed.; Plenum: New York, 1997; pp 237−261.
(14) Majewska-Sawka, A.; Nothnagel, E. A. The multiple roles of arabinogalactan proteins in plant development. *Plant Physiol.* **2000**, *122*, 3−10.
(15) Loosveld, A. M. A.; Grobet, P. J.; Delcour, J. A. Contents and structural features of water-extractable arabinogalactan in wheat flour fractions. *J. Agric. Food Chem.* **1997**, *45*, 1998−2002.
(16) Simmonds, D. H.; O'Brien, T. P. Morphological and biochemical development of the wheat endosperm. In *Advances in Cereal Science and Technology*; Pomeranz, Y., Ed.; American Association of Cereal Chemists: St. Paul, MN, 1981; Vol. IV, pp 5−70.
(17) Rogers, S. O.; Quatrano, R. S. A quantitative analysis of some ultrastructural aspects of seed development of wheat caryopsis. *Am. J. Bot.* **1983**, *70*, 308−311.

(18) Lopes, M. A.; Larkins, B. A. Endosperm origin, development, and function. *Plant Cell* **1993**, *5*, 1383−1399.
(19) Berger, F. Endosperm development. *Curr. Opin. Plant Biol.* **1999**, *2*, 28−32.
(20) Guillon, F.; Tranquet, O.; Quillien, L.; Utille, J.-P.; Ordaz Ortiz, J. J.; Saulnier, L. Generation of polyclonal and monoclonal antibodies against arabinoxylans and their use for immunocytochemical location of arabinoxylans in cell walls of endosperm of wheat. *J. Cereal Sci.* **2004**, *40*, 167−182.
(21) Philippe, S.; Saulnier, L.; Guillon, F. Arabinoxylans and β-glucans deposition in cell wall during wheat endosperm development. *Planta*, on line.
(22) Piot, O.; Autran, J.-C.; Manfait, M. Spatial distribution of protein and phenolic constituents in wheat grain as probed by confocal Raman spectroscopy. *J. Cereal Sci.* **2000**, *32*, 57−71.
(23) Piot, O.; Autran, J.-C.; Manfait, M. Investigation by confocal Raman microspectroscopy of the molecular factors responsible for grain cohesion in the triticum aestivum bread wheat. Role of the cell walls in the starchy endosperm. *J. Cereal Sci.* **2001**, *34*, 191−205.
(24) Barron, C.; Parker, M. L.; Mills, E. N. C.; Rouau, X.; Wilson, R. H. FTIR imaging of wheat endosperm cell walls *in situ* reveals compositional and architectural heterogeneity related to grain hardness. *Planta* **2005**, *220*, 667−677.
(25) Agarwal, U. P.; Atalla, R. H. In situ Raman microprobes studies of plant cell walls: Macromolecular organization and compositional variability in the secondary wall of *Picea mariana* (mill.) B.S.P. *Planta* **1986**, *169*, 325−332.
(26) Atalla, R. H.; Agarwal, U. P. Recording Raman spectra from plant cell walls. *J. Raman Spectrosc.* **1986**, *17*, 229−231.
(27) Séné, C. F. B.; McCann, M. C.; Wilson, R. H.; Grinter, R. Fourrier-transform Raman and Fourier transform infrared spectroscopy−An investigation of 5 higher plant cell-walls and their components. *Plant Physiol.* **1994**, *106*, 1623−1631.
(28) McCann, M. C.; Chen, L.; Roberts, K.; Kemsley, E. K.; Séné, C.; Carpita, N. C.; Stacey, N. J.; Wilson, R. H. Infrared microspectroscopy: Sampling heterogeneity in plant cell wall composition and architecture. *Physiol. Plant* **1997**, *100*, 729−738.
(29) Chen, L.; Carpita, N. C.; Reiter, W. D.; Wilson, R. H.; Jeffries, C.; McCann, M. C. A rapid method to screen cell wall mutants using discriminant analysis of Fourier transform infrared spectra. *Plant J.* **1998**, *16*, 385−392.
(30) Robert, P.; Marquis, M.; Barron, C.; Guillon, F.; Saulnier, L. FT-IR Investigation of cell wall polysaccharides from cereal grains. Arabinoxylan infrared assignment. *J. Sci. Food Agric.* **2005**, *53*, 7014−7018.
(31) McMaster, G. S.; Wilhem, W. W. Growing degree-days: One equation, two interpretations. *Agric. For. Meteorol.* **1997**, *87*, 291−300.
(32) Savitzky, A.; Golay, M. J. Smoothing and differentiation of data by simplified least-squares procedures. *Anal. Chem.* **1964**, *36*, 1627−1639.
(33) Cowe, I. A.; McNicol, J. W. The use of principal component in the analysis of near-infrared spectra. *Appl. Spectrosc.* **1985**, *39*, 257−265.
(34) Robert, P.; Devaux, M.-F.; Bertrand, D. Beyond prediction: extracting relevant information from near-infrared spectra. *J. Near Infrared Spectrosc.* **1996**, *4*, 75−84.
(35) Marchessault, R. H.; Liang, C. Y. The infrared spectra of crystalline polysaccharides. VIII. Xylans. *J. Polym. Sci.* **1962**, *59*, 357−378.
(36) Kacurakova, M.; Ebringerova, A.; Hirsch, J.; Hromadkova, Z. Infrared study of arabinoxylans. *J. Sci. Food Agric.* **1994**, *66*, 423−427.
(37) Kacurakova, M.; Wellner, N.; Ebringerova, A.; Hromadkova, Z.; Wilson, R. H.; Belton, P. S. Characterisation of xylan-type polysaccharides and associated cell wall components by FT-IR and FT-Raman spectroscopies. *Food Hydrocolloids* **1999**, *13*, 35−41.
(38) Kacurakova, M.; Capek, P.; Sasinkova, V.; Wellner, N.; Ebringerova, A. FT-IR study of plant cell wall model compounds: Pectic polysaccharides and hemicelluloses. *Carbohydr. Polym.* **2000**, *43*, 195−203.
(39) Coles, G. Relationship of mixed-link beta-glucan accumulation to accumulation of free sugars and others glucans in the developing barley endosperm. *Carlsberg Res. Commun.* **1979**, *44*, 439−453.
(40) Carpita, N. C.; Defernez, M.; Findlay, K.; Wells, B.; Shoue, D. A.; Catchpole, G.; Wilson, R. H.; McCann, M. C. Cell wall architecture of the elongating maize coleoptile. *Plant Physiol.* **2001**, *127*, 551−565.
(41) Trethewey, J. A. K.; Harris, P. J. Location of (1-3)- and (1-3),-(1-4)-β-D-glucans in vegetative cell walls of barley (*Hordeum vulgare*) using immunogold labeling. *New Phytol.* **2002**, *154* (2), 347−358.
(42) Meier, H.; Reid, J. S. G. Reserve polysaccharides other than starch in higher plants. In *Encyclopedia of Plant Physiology*; Loewus, A. F. A., Tanner, W., Eds.; Springer-Verlag: Berlin, 1982; Vol. 13, pp 418−471.
(43) Izydorczyk, M. S.; McGregor, A. W. Evidence of intermolecular interactions of b-glucans and arabinoxylans. *Carbohydr. Polym.* **2000**, *41*, 417−420.
(44) Lee, R. C.; Burton, R. A.; Hrmova, M.; Fincher, G. B. Barley arabinoxylan arabinofuranohydrolases: Purification, characterization and determination of primary structures from cDNA clones. *Biochem. J.* **2001**, *356*, 181−189.
(45) Gibeaut, D. M.; Pauly, M.; Bacic, A.; Fincher, G. F. Changes in cell wall polysaccharides in developing barley (Hordeum vulgare) coleoptiles. *Planta* **2005**, *221*, 729−738.
(46) Gibeaut, D. M.; Carpita, N. C. Tracing cell wall biogenesis in intact cells and plant: Selective turnover and alteration of soluble and cell wall polysaccharides in grasses. *Plant Physiol.* **1991**, *97*, 551−561.
(47) McClintock, B. Development of the maize endosperm revealed by clones. In *The Clonal Basis of Development*; Subtelny, S., Ed.; Academic Press: New York, 1978; pp 217−237.
(48) Wetzel, D. L.; Reffner, J. A. Using spatially resolved Fourier transform infrared microbeam spectroscopy to examine microstructure of wheat kernels. *Cereal Foods World* **1993**, *38*, 9−20.
(49) Yu, P.; McKinnon, J. J.; Christensen, C. R.; Christensen, D. A. Imaging molecular chemistry of Pioneer corn. *J. Agric. Food Chem.* **2004**, *52*, 7345−7352.

Received for review November 23, 2005. Revised manuscript received January 30, 2006. Accepted January 31, 2006.

JF052922X